

Effect of GGA on the half-metallicity of the itinerant ferromagnet CoS_2

Tatsuya Shishidou and A. J. Freeman

Department of Physics and Astronomy, Northwestern University, Evanston, Illinois 60208

Ryoji Asahi

Toyota Central R&D Laboratories, Inc., Nagakute, Aichi 480-1192, Japan

(Received 7 May 2001; published 1 October 2001)

The half-metallicity of CoS_2 , important for its possible use in spintronic applications, is investigated by means of density functional full-potential linearized augmented plane wave calculations within both the local spin-density approximation (LSDA) and the generalized gradient approximation (GGA). In contrast with earlier and our own predictions employing the LSDA, we find that CoS_2 is clearly half-metallic with use of the GGA for the exchange-correlation functional. While the GGA induced modifications of the band structure are significant, they are limited to only the $e_{g\downarrow}$ state which is responsible for producing the half-metallicity, while leaving all other features the same as those obtained by LSDA. We address the recently measured reflectivity spectra and rectify the assignments given for their underlying optical transitions.

DOI: 10.1103/PhysRevB.64.180401

PACS number(s): 75.50.Cc, 71.20.Be, 72.25.Ba

Recently, half-metallic ferromagnets are attracting increasing attention since a high degree of spin polarization is expected for the conducting current, which is necessary for the new class of industrial applications—called “spintronics.”^{1,2} Pyrite-type CoS_2 , a ferromagnetic metal, is receiving revived interest with a focus on its possible half-metallicity.^{3–6} While the relatively low T_C of CoS_2 , 120 K, makes it difficult to exploit CoS_2 for practical applications, it is still much higher than liquid- N_2 temperature so that CoS_2 can be utilized as laboratory instruments. Kirczenow⁶ proposed theoretically that an interface between CoS_2 and a semiconductor is a promising candidate for ideal spin filters even if CoS_2 is not half-metallic. Now, its possible half-metallicity may be seen to follow from a simple consideration of its valence as $\text{Co}^{2+}(\text{S}_2)^{2-}$ that gives a $3d^7$ electron configuration. Since the crystal field is so strong that the $3d$ state is in the low-spin state with fully occupied t_{2g} states: $t_{2g}^6 e_g^1$ ($S = 1/2$), only one e_g electron is responsible for the magnetism. If the occupation of the e_g state in the metal is restricted to the majority-spin state, then in this simple picture, CoS_2 is a half-metallic ferromagnet.

Although CoS_2 has been extensively studied, there still exists a contradiction about its electronic structure. Dynamical susceptibility measurements showed that CoS_2 is classified as an itinerant ferromagnet.⁷ However, a magnetic form factor analysis showed that the magnetic moment distribution is localized on the Co atoms.⁸ Photoemission spectroscopy showed slight spectral changes between the paramagnetic and ferromagnetic phases.^{3,9} Takahashi *et al.*³ interpreted this change with supposing that the $e_{g\downarrow}$ band is partially filled in the ferromagnetic phase. On the other hand, Yamamoto *et al.*⁴ measured reflectivity spectra and found significant changes at T_C ; from a fitting analysis, they concluded that CoS_2 is half-metallic with the $e_{g\downarrow}$ state located far above E_F .

While several first-principles calculations based on the local spin-density approximation (LSDA) to density functional theory have been attempted to study CoS_2 , none of them

shows that it is half-metallic: A linear combination of atomic orbitals (LCAO) approach by Zhao *et al.*¹⁰ showed that CoS_2 just misses being half-metallic, i.e., a small portion of the $e_{g\downarrow}$ state is occupied. Using the linear muffin-tin orbital (LMTO) method with the atomic sphere approximation, Yamada *et al.*¹¹ argued that CoS_2 is a normal metal whereas Kwon *et al.*⁵ showed that it is nearly half-metallic in accordance with the result by Zhao *et al.*

To address the uncertainty among the first-principles calculations and to examine the possible half-metallicity of CoS_2 , we performed band-structure calculations by the highly precise full-potential linearized augmented plane wave¹² (FLAPW) method. In addition to employing the LSDA for the exchange-correlation (XC) functional, we examined the effect of the generalized gradient approximation (GGA) correction. We show that the GGA greatly modifies the band structure of CoS_2 and results in a half-metallic ground state. The origin of this change may be explained in terms of the anisotropic GGA correction to the XC potential, which pushes up only the $e_{g\downarrow}$ state relevant to the half-metallicity.

For the calculations, we adopt the Hedin-Lundqvist parameterization¹³ for the LSDA XC functional and the GGA formula of Perdew *et al.*¹⁴ Core states were treated fully relativistically and valence states scalar relativistically. Muffin-tin (MT) sphere radii were chosen to be 2.3 and 1.9 a.u. for Co and S, respectively. The cutoff of the plane-wave basis was 12.3 Ry, producing about 830 plane waves and a star-function cutoff of 100 Ry. Spherical harmonics with $l \leq 8$ were used inside the MT spheres. The k -point summation was performed by the tetrahedron method using 119 k -points in the irreducible wedge. The unit cell contains four Co atoms and eight S atoms, for which we have used the experimental lattice parameters, $a = 5.524 \text{ \AA}$ and $u = 0.389$.¹⁵

The density of states (DOS) calculated within the LSDA is displayed in Fig. 1. Molecular-orbital states, originating from the dimerization of S atoms, are seen at the deepest binding energy: $3s\sigma$ (bonding) and $3s\sigma^*$ (antibonding) states at -16 and -13 eV , respectively. $3p$ valence bands

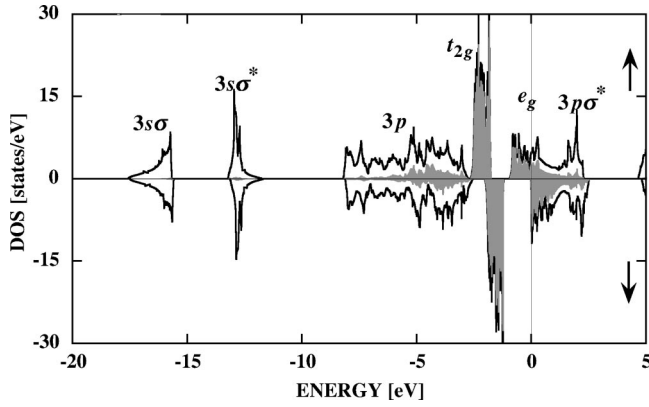


FIG. 1. Spin-projected LSDA DOS. The shaded area represents the Co 3d states.

are very broad and spread out between -8 and -3 eV. Around E_F , there exist exchange-split Co 3d states. At about 2 eV, $3p\sigma^*$ states of the S-S dimer are clearly seen. We should mention differences with the LCAO and LMTO calculations which give deeper energy positions for the S-related occupied states than does the present FLAPW calculation by about 2 eV. Since the pyrite structure is far from close-packed and the packing fraction by the touching spheres is only 43.5%,¹¹ we believe it is crucial to treat the interstitial region in a reasonable way—for instance, using plane waves. In addition, the full-potential method is preferable for a better description of the uniaxial S-S dimers.

Band dispersion¹⁶ around E_F for the spin-up (majority) state is shown in Fig. 2. The t_{2g} bands are narrow and fully occupied. The e_g bands are relatively broad and well hybridized with the S $3p$ states. The LSDA and GGA dispersions are astonishingly identical with each other: only small energy differences (<0.1 eV) are seen for the t_{2g} and $3p\sigma^*$ bands. The band dispersion for the spin-down (minority) state is displayed in Fig. 3. With the LSDA [Fig. 3(a)], a small electron pocket is formed around the R point (indicated by circles in the figure) that destroys the half-metallicity. Unlike the case of the spin-up dispersion, the effect of the GGA correction is dramatic [Fig. 3(b)]. Although the occupied t_{2g} bands are not changed significantly, the unoccupied e_g - $3p$

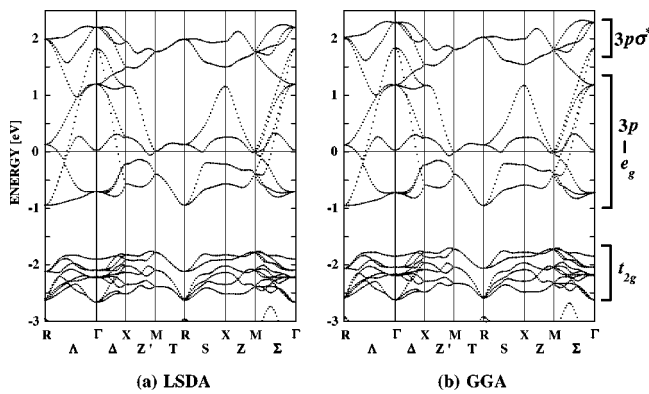


FIG. 2. Majority-spin band dispersion by the (a) LSDA and (b) GGA. Notation of high-symmetry k -points and lines is from Zhao *et al.* (Ref. 10).

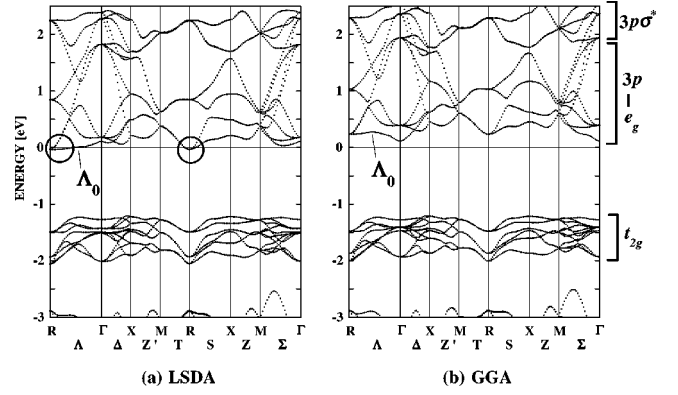


FIG. 3. Same as Fig. 2 but for minority spin. See text for details.

hybridized bands and $3p\sigma^*$ bands are pushed up in energy by between 0 and 0.3 eV.

The most prominent and enlightening change in Fig. 3 is seen for the band indicated as Λ_0 from R through Γ . For a clear comparison, we display the calculated LSDA and GGA Λ_0 bands in Fig. 4. Around the R point, the eigenvalue shifts are quite large, about 0.3 eV, and its wave functions contain a lot of the Co e_g component with a weight of about 80%. On the other hand, the eigenvalue shift at Γ is almost zero, 8 meV, and its wave function has no Co 3d character. Thus it can be said that the effect of the GGA is very significant but limited to only the $e_{g\downarrow}$ state.

In Fig. 5, the LSDA and GGA DOS's are blown up just around E_F . In the LSDA DOS, 0.006 electrons/CoS₂ are occupied in the spin-down state due to the electron-pocket formation seen in Fig. 3(a). With the GGA, there is no spin-down DOS at E_F : it is clearly half-metallic with the relevant states pushed up by about 0.2 eV.

Now, let us raise a question: what is the origin of the eigenvalue shift for the $e_{g\downarrow}$ state? The GGA exchange energy¹⁷ has an enhancement factor compared to the LSDA, which is a function of the scaled density gradient given by

$$s = \frac{|\nabla n|}{2k_F n} = \frac{1}{2(3\pi^2)^{1/3}} \frac{|\nabla n|}{n^{4/3}}, \quad (1)$$

where n is the electron density of each spin. If s becomes larger, the GGA can gain exchange energy. The self-consistent LSDA valence-electron density is plotted in Fig.

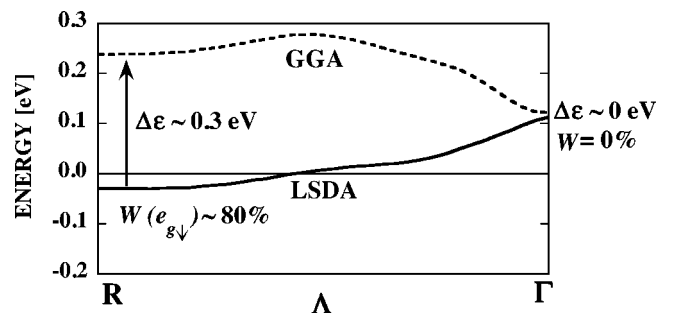


FIG. 4. Comparison of the dispersion of the minority Λ_0 band between the LSDA (solid line) and GGA (broken line). See text for details.

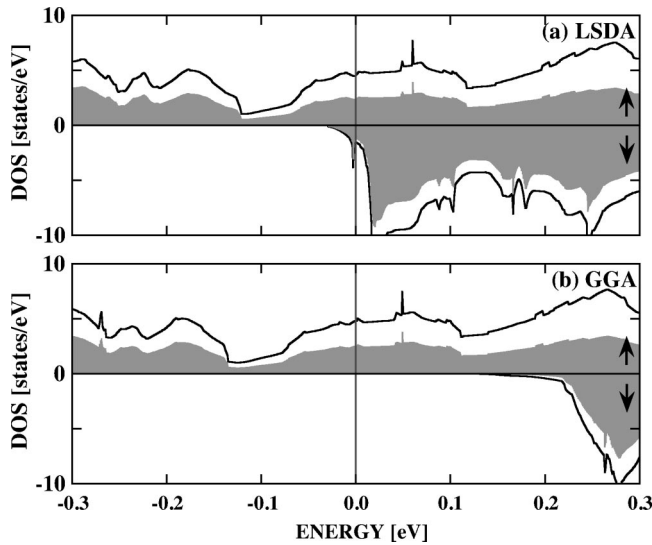


FIG. 5. DOS's just around E_F to examine the half-metallicity calculated by the (a) LSDA and (b) GGA. The shaded area represents the Co 3d state.

6. A section of the (110) plane is shown, where we can see both the Co-S bond and S-S dimerization. The spin-up density n_\uparrow contains, in addition to the fully occupied t_{2g} electrons, a large number of the e_g electrons whose wave function is extended along the Co-S direction. Thus n_\uparrow is quite spherical around the Co nucleus and we can notice the contribution of the e_g electrons to the Co-S bond.

In the case of the LSDA spin-down density, however, we have only a few e_g electrons so that n_\downarrow around the Co nucleus is rather aspherical (close to the t_{2g} symmetry) with a strong depression along the Co-S direction. If we can expel the small number of $e_{g\downarrow}$ electrons from the occupied state, the following changes are expected around the Co nucleus in the Co-S direction: the angular gradient of n_\downarrow [numerator of Eq. (1)] will be magnified with a more emphasized depression (complete t_{2g} symmetry); n_\downarrow will be smaller [denomi-

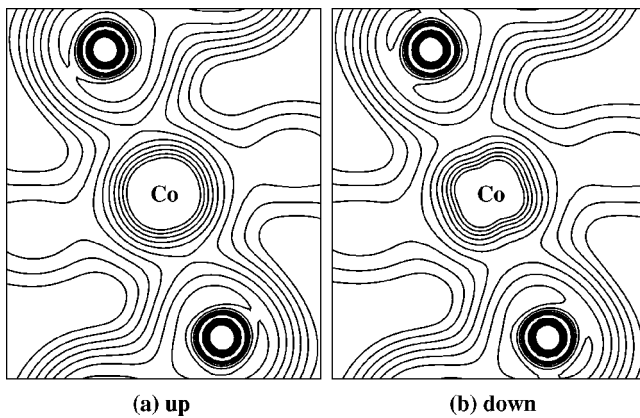


FIG. 6. Contour map of the LSDA valence charge density plotted in the (110) plane passing through both Co-S and S-S bonds: (a) spin-up and (b) spin-down density. Successive contours are given by $n_0 p^{m-1}$ with $n_0 = 0.01$ electron/a.u.,³ $p = 1.4$, and $m = 1, 2, \dots, 10$. The frame height is equal to the lattice constant.

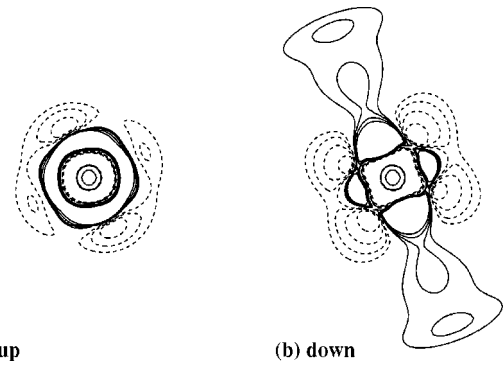


FIG. 7. Contour map of $\Delta V_{xc} = V_{xc}^{GGA} - V_{xc}^{LSDA}$ for the Co atomic region in the same plane as Fig. 6, for the (a) spin-up and (b) spin-down state. Positive (full line) and negative (broken line) contours are drawn at ± 0.4 , ± 0.6 , ± 0.9 , and ± 1.35 eV. The frame height is 4 a.u.

nator of Eq. (1)] and consequently the scaled density gradient s will be larger. Thus a GGA modification for the spin-down state is expected along the Co-S bonding direction in order to exclude the $e_{g\downarrow}$ electrons and gain exchange energy.

To confirm this reasoning, we plot in Fig. 7 the difference of the XC potential, $\Delta V_{xc} = V_{xc}^{GGA} - V_{xc}^{LSDA}$, for the region of the Co MT sphere. Here, V_{xc}^{GGA} was obtained by a single iteration GGA calculation from the converged LSDA density (note that the inputs for calculating V_{xc} are the same for LSDA and GGA). For the spin-up state, the GGA correction is not significant. In the case of the spin-down state, however, the O_h symmetry is emphasized by the GGA, and an especially strong repulsive potential for the e_g state is achieved in the large region that spreads to the neighboring S atoms. This is the origin of the eigenvalue shift for the $e_{g\downarrow}$ state which we have seen in Figs. 3 and 4. It should be noted that employing the full-potential method is essential in order to have such an anisotropic GGA modification as presented in Fig. 7(b).

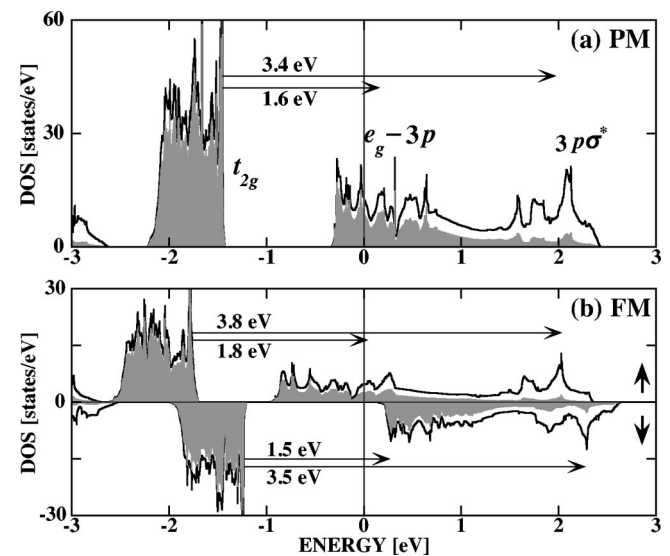


FIG. 8. GGA DOS's for the (a) paramagnetic and (b) ferromagnetic phases. Supposed optical transitions for the reflectivity spectra (Ref. 4) are indicated by arrows.

We briefly mention the recently measured reflectivity spectra, where significant spectral changes were observed between the paramagnetic (PM) and ferromagnetic (FM) phases.⁴ Above T_C , there are two peaks in the spectrum located at 1.6 and 3.4 eV, which were assigned to the $t_{2g} - e_g$ and $t_{2g} - 3p^*$ optical transitions, respectively; these correspond well with the results of the present calculation [See Fig. 8(a)]. Below T_C , the spectrum becomes broad with no clear peak. Yamamoto *et al.*⁴ performed a fitting analysis and argued that there are two transitions: the $t_{2g} - e_g$ transition in the spin-up channel at 1.5 eV followed by the $t_{2g} - 3p^*$ in the spin-down channel at 2.6 eV. This is strongly inconsistent with the expected transitions from our calculation — below 2 eV, the $t_{2g} - e_g$ transition should occur in *both spin channels* (1.5 eV in the spin-down and 1.8 eV in up) and there are in all *at least four* transitions [Fig. 8 (b)]. The broad spectral feature observed in the FM phase may originate from the spin-down $t_{2g} \rightarrow e_g$ transition since the $e_{g\downarrow}$ DOS remains relatively high well above threshold. In addition, the spin-up $e_g \rightarrow 3p^*$ transition (not indicated in the figure) might contribute to the observed broad spectral feature. Now, Yamamoto *et al.* assumed only two oscillator strengths in the fitting procedure and this may be the main

reason why they reached such a simplified, and hence, inadequate picture for the FM phase.

In conclusion, we have investigated the half-metallicity of CoS₂ with highly precise first-principles FLAPW calculations. The LSDA calculation shows that CoS₂ just misses being a half-metal in accordance with some of previous calculations.^{5,10} With the GGA, however, it is clearly half-metallic with only the $e_{g\downarrow}$ states pushed up in energy. Clearly, experimental investigations into the half-metallicity of CoS₂ with the Andreev reflection technique¹⁸ are highly desirable. The present result strongly contrasts with the GGA implementation for the itinerant ferromagnet Fe, where the energetic stability among various structures is greatly improved by the GGA while no significant change is seen for the DOS (the LSDA is good enough to give the correct band structure of Fe).¹⁹ Although CoS₂ is an itinerant ferromagnet, the GGA effect appears to be rather similar to those for strongly correlated transition-metal oxides.^{20,21}

We thank W. Mannstadt, J. Medvedeva, Y. J. Zhao, and K. Nakamura for assistance. Work was supported in part by a grant of HPC resources from the Arctic Region Supercomputing Center.

-
- ¹G.A. Prinz, Phys. Today **48** (4), 58 (1995).
²K.-I. Kobayashi, T. Kimura, H. Sawada, K. Terakura, and Y. Tokura, Nature (London) **395**, 677 (1998).
³T. Takahashi, Y. Naitoh, T. Sato, T. Kamiyama, K. Yamada, H. Hiraka, Y. Endoh, M. Usuda, and N. Hamada, Phys. Rev. B **63**, 094415 (2001).
⁴R. Yamamoto, A. Machida, Y. Moritomo, and A. Nakamura, Phys. Rev. B **59**, R7793 (1999).
⁵S.K. Kwon, S.J. Youn, and B.I. Min, Phys. Rev. B **62**, 357 (2000).
⁶G. Kirczenow, Phys. Rev. B **63**, 054422 (2001).
⁷H. Hiraka, Y. Endoh, and K. Yamada, J. Phys. Soc. Jpn. **66**, 818 (1997).
⁸A. Ohsawa, Y. Yamaguchi, H. Watanabe, and H. Itoh, J. Phys. Soc. Jpn. **40**, 986 (1976).
⁹T. Muro, A. Kimura, T. Iwasaki, S. Ueda, S. Imada, T. Matsushita, A. Sekiyama, T. Susaki, K. Mamiya, T. Harada, T. Kanomata, and S. Suga, J. Electron Spectrosc. Relat. Phenom. **88**, 91 (1998).
¹⁰G.L. Zhao, J. Callaway, and M. Hayashibara, Phys. Rev. B **48**, 15 781 (1993).
¹¹H. Yamada, K. Terao, and M. Aoki, J. Magn. Magn. Mater. **177-181**, 607 (1998).
¹²E. Wimmer, H. Krakauer, M. Weinert, and A.J. Freeman, Phys. Rev. B **24**, 864 (1981); M. Weinert, E. Wimmer, and A.J. Freeman, *ibid.* **26**, 4571 (1982); H.J.F. Jansen and A.J. Freeman, *ibid.* **30**, 561 (1984).
¹³L. Hedin and B.I. Lundqvist, J. Phys. C **4**, 2064 (1971); U. von Barth and L. Hedin, *ibid.* **5**, 1629 (1972).
¹⁴J.P. Perdew, K. Burke, and M. Ernzerhof, Phys. Rev. Lett. **77**, 3865 (1996).
¹⁵R.W.G. Wyckoff, *Crystal Structures* (Interscience, New York, 1965), Vol. 1.
¹⁶Our band dispersion by the LSDA is much different from the LCAO one given in Ref. 10. We have confirmed the validity of our calculation by another FLAPW package coded by T. Oguchi, which is based on the formalism of J.M. Soler, and A.R. Williams, Phys. Rev. B **40**, 1560 (1989).
¹⁷J.P. Perdew, J.A. Chevary, S.H. Vosko, K.A. Jackson, M.R. Pederson, D.J. Singh, and C. Fiolhais, Phys. Rev. B **46**, 6671 (1992).
¹⁸R.J. Soulen, J.M. Byers, M.S. Osofsky, B. Nadgorny, T. Ambrose, S.F. Cheng, P.R. Broussard, C.T. Tanaka, J. Nowak, J.S. Moodera, A. Barry, and J.M.D. Coey, Science **282**, 85 (1998).
¹⁹T.C. Leung, C.T. Chan, and B.N. Harmon, Phys. Rev. B **44**, 2923 (1991); D.J. Singh, W.E. Pickett, and H. Krakauer, *ibid.* **43**, 11 628 (1991).
²⁰P. Dufek, P. Blaha, V. Sliwko, and K. Schwarz, Phys. Rev. B **49**, 10 170 (1994).
²¹H. Sawada, N. Hamada, K. Terakura, and T. Asada, Phys. Rev. B **53**, 12 742 (1996).